

# Dependence of deformation of a plate on the subsoil in relation to the parameters of the 3D model

R. Cajka, J. Labudkova

**Abstract**—The purpose of this paper is to compare the measured subsidence of the foundation in experiments based on FEM calculations.

This paper describes how calculated deformations depend on parameters of soil environment modelled by 3D finite elements. When using 3D elements for creation of a 3D model, it is, in particular, essential to choose correctly the size of the model area which represents the subsoil, the boundary conditions and the size of the finite element network. The parametric study evaluates impacts of those parameters on final deformation.

**Keywords**—Foundation structure, soil – structure interaction, contact stress, 3D FEM element

## I. INTRODUCTION

Because calculated subsidence and real subsidence of foundations do not correlate well, a site survey is needed and experimental measurements are carried out in order to determine subsidence of foundation soil under structures, deformation of foundation slabs and characteristics of stress in foundation slabs which depend on parameters of subsoil. Using results of such experiments, the methods used for calculation of subsidence are modified and become more strict. In 2010, testing equipment – a stand – was erected in the Faculty of Civil Engineering, VSB – Technical University of Ostrava.



Fig. 1 Testing equipment – the stand

R. Cajka, Professor, Department of Structures, Faculty of Civil Engineering, VSB – Technical University of Ostrava, Ludvika Podeste 1875/17, 708 33 Ostrava-Poruba, radim.cajka@vsb.cz

J. Labudkova, Bachelor, Department of Structures, Faculty of Civil Engineering, VSB – Technical University of Ostrava, Ludvika Podeste 1875/17, 708 33 Ostrava-Poruba, jana.labudkova@vsb.cz

The stand measures deformation and monitors interaction between stress and deformation. In 2012 an experiment was carried out using the stand.

Numerical calculations were performed in different software applications. Values measured during the load tests were compared with values calculated by means of interaction FEM models with 3D element of subsoil. The calculations were carried out for several sizes of the subsoil and for different boundary conditions. The values were compared then and impacts on final deformation and internal forces in the foundation structure were evaluated.

## II. DESCRIPTION OF THE TASK – A CONCRETE SLAB ON SUBSOIL LOADED IN A CENTRE

A sample used for the experiment and for monitoring of foundation – subsoil interaction was a prefabricated concrete tile 500 x 500 x 48 mm.

The modulus of elasticity of concrete  $E$  is 36.3 GPa and Poisson coefficient is  $\nu = 0.2$ . The upper layer of subsoil consists of loess loam with F4 consistency. Thickness of that layer is about 5 meters.



Fig. 2 Test sample

Volumetric weight of soil is  $\gamma = 18.5 \text{ kN.m}^{-3}$ , Poisson coefficient is  $\nu = 0.35$ , static Young's modulus is  $E_{\text{DEF}} = 2.65 \text{ MPa}$  and oedometric modulus of elasticity is  $E_{\text{OED}} = 4.27 \text{ MPa}$ . From the geologic point of view, foundation soil is not complex.

During the test, the concrete slab was loaded in the centre by the pressure applied by a hydraulic press. Dimensions of the area under load were 100 x 100 mm.



Fig. 3 Load test

The loading was performed in an even velocity until the sample failed— this occurred after 85 s. The load at the moment of failure was 18.640 kN.



Fig. 4 Failure of the slab

III. CREATING A COMPUTATIONAL MODEL IN ANSYS

The computational model was created using a 2D element SHELL 181 for the slab and a 3D element SOLID 45 for the model of subsoil.

Shell 181 is a four-node element with six degrees of freedom in a node. The degrees of freedom represent three dislocations in x, y and z axes and three torsional displacements around x, y and z axes. SOLID 45 is defined by eight nodes where each node is characterised by three degrees of freedom (dislocations of the node in x, y and z axes).

Dead weight of soil and concrete slab were not considered for the calculation. The size of three-side or four-side elements in the slab network is 0.025 x 0.025 m. When creating a 3D model, the chosen finite elements in the network are tetrahedral or hexahedral and their size is 0.10 x 0.10 x 0.10 m. The load of 18,640 N is applied in a centre onto the 100 x 100 mm area. This is modelled in several points of the network model. Calculation is made on the basis of the number of load nodes.

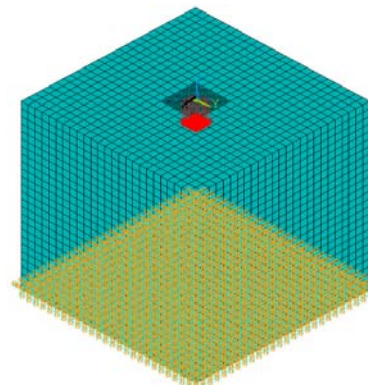


Fig. 5 Model created in ANSYS

Contact elements are used to solve this interaction task. The contact elements represent surfaces of elements in mutual contact and monitor kinematics of deformation. The contact is intermediated by a contact pair TARGE170 - CONTA173 which is used for modeling of 3D tasks.

IV. COMPARING DIFFERENT MODELS IN TERMS OF IMPACTS ON DEFORMATION

Four aspects were considered when comparing different models. One aspect is dependence of deformation on the variant boundary conditions. The second aspect is dependence of deformation on variable depth of the subsoil, while keeping the same ground plan of the subsoil. The third aspect is dependence of deformation on variable size of ground plan of the subsoil, while keeping the same depth. The last aspect is dependence of deformation on the total size of modelled area.

The comparison was made for four different boundary conditions - see Fig. 7.

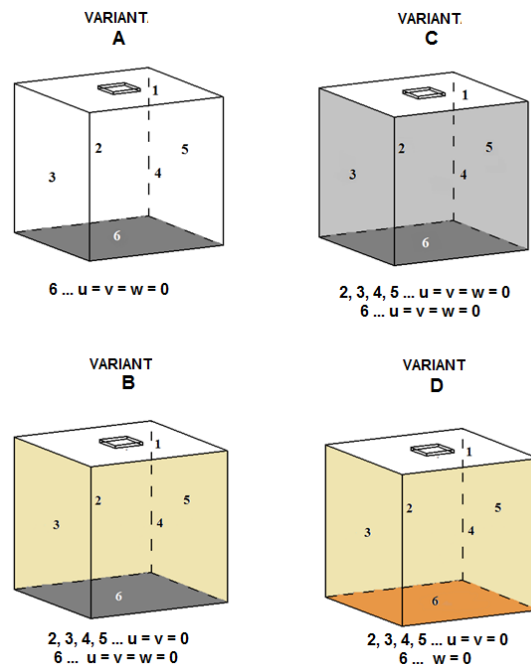


Fig. 6 Different boundary conditions

**A. Deformation vs. boundary conditions**

For this comparison, the same size of the subsoil model is used for all types of the boundary conditions. The first subsoil model had the size 2.5 x 2.5 x 2.5 m. The table and chart below shows differences in the vertical deformation for different types of the boundary conditions.

Dimensions of the soil model [m]	Boundary conditions	Size of the element [m x m x m]	Resulting vertical deformation w [mm]
2,5 x 2,5 x 2,5	A	0,1 x 0,1 x 0,1	9,984
2,5 x 2,5 x 2,5	B		8,848
2,5 x 2,5 x 2,5	C		8,420
2,5 x 2,5 x 2,5	D		8,848

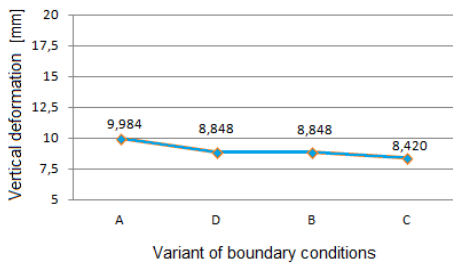


Fig. 7 Vertical deformations vs. boundary conditions; 2.5 x 2.5 x 2.5 m

For the subsoil model with the dimensions of 2.5 x 2.5 x 5.0 m the differences in the vertical deformations calculated for different boundary conditions are as follows:

Dimensions of the soil model [m]	Boundary conditions	Size of the element [m x m x m]	Resulting vertical deformation w [mm]
2,5 x 2,5 x 5	A	0,1 x 0,1 x 0,1	12,832
2,5 x 2,5 x 5	B		10,602
2,5 x 2,5 x 5	C		8,486
2,5 x 2,5 x 5	D		10,602

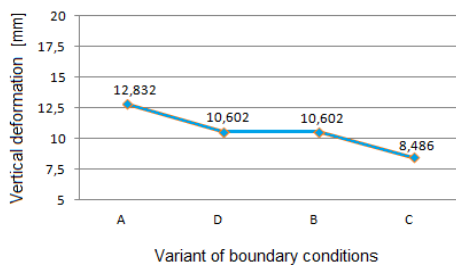


Fig. 8 Vertical deformations vs. boundary conditions; 2.5 x 2.5 x 5.0 m

For the subsoil model with the dimensions of 2.5 x 2.5 x 7.5 m the differences in the vertical deformations calculated for different boundary conditions are as follows:

Dimensions of the soil model [m]	Boundary conditions	Size of the element [m x m x m]	Resulting vertical deformation w [mm]
2,5 x 2,5 x 7,5	A	0,1 x 0,1 x 0,1	15,645
2,5 x 2,5 x 7,5	B		12,355
2,5 x 2,5 x 7,5	C		8,486
2,5 x 2,5 x 7,5	D		12,355

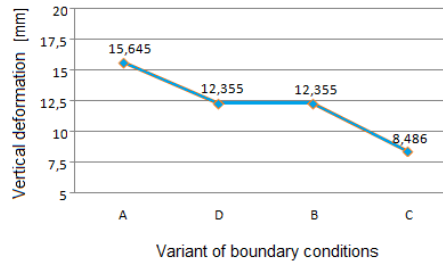


Fig. 9 Vertical deformations vs. boundary conditions; 2.5 x 2.5 x 7.5 m

**B. Deformation versus variable depth of the subsoil model**

When the ground plan is 2.5 x 2.5 m and boundary conditions are A:

Dimensions of the soil model [m]	Boundary conditions	Size of the element [m x m x m]	Resulting vertical deformation w [mm]
2,5 x 2,5 x 2,5	A	0,1 x 0,1 x 0,1	9,984
2,5 x 2,5 x 5,0			12,832
2,5 x 2,5 x 7,5			15,645

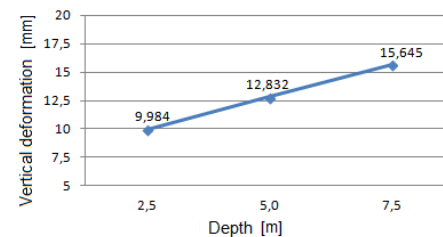


Fig. 10 Variant A – the resulting vertical deformation and vertical deformation vs. depth

When the ground plan is 2.5 x 2.5 m and boundary conditions are B:

Dimensions of the soil model [m]	Boundary conditions	Size of the element [m x m x m]	Resulting vertical deformation w [mm]
2,5 x 2,5 x 2,5	B	0,1 x 0,1 x 0,1	8,848
2,5 x 2,5 x 5,5			10,602
2,5 x 2,5 x 7,5			12,355

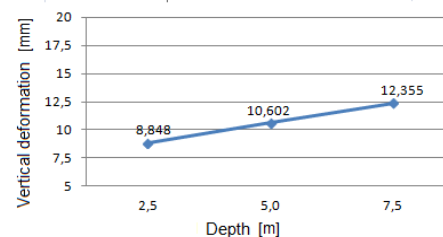


Fig. 11 Variant B – the resulting vertical deformation and vertical deformation vs. depth

When the ground plan is 2.5 x 2.5 m and boundary conditions are C:

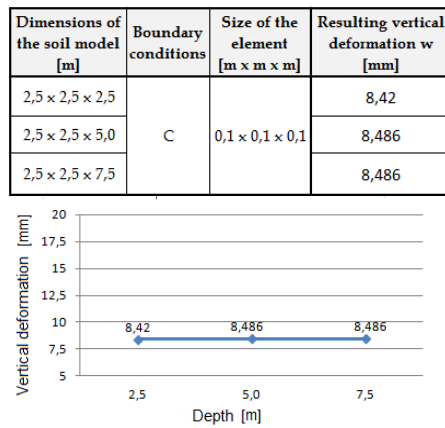


Fig. 12 Variant C – the resulting vertical deformation and vertical deformation vs. depth

When the ground plan is 2.5 x 2.5 m and boundary conditions are D:

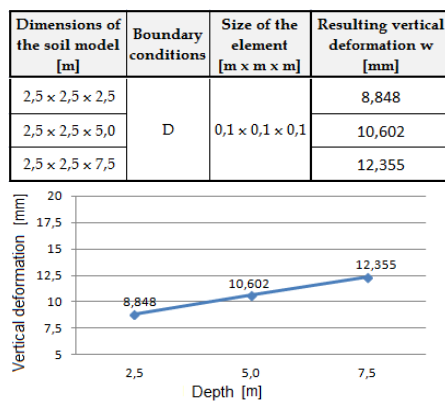


Fig. 13 Variant D – the resulting vertical deformation and vertical deformation vs. depth

C. Deformation versus variable ground plan of the subsoil

When the depth is 2.5 m and boundary conditions are A:

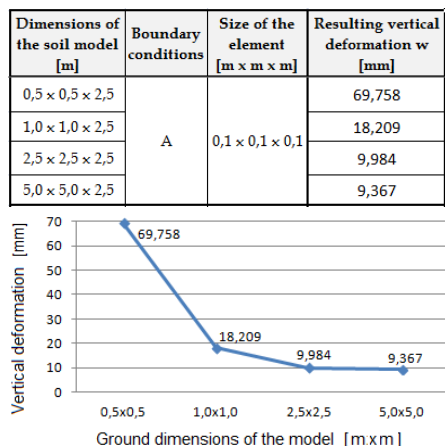


Fig. 14 Variant A – the resulting vertical deformation and vertical deformation vs. ground plan of the model

When the depth is 2.5 m and boundary conditions are B:

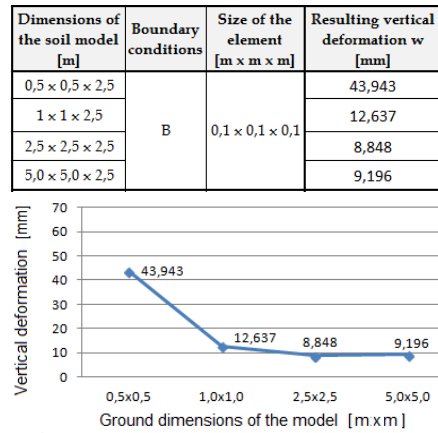


Fig. 15 Variant B – the resulting vertical deformation and vertical deformation vs. ground plan of the model

When the depth is 2.5 m and boundary conditions are C:

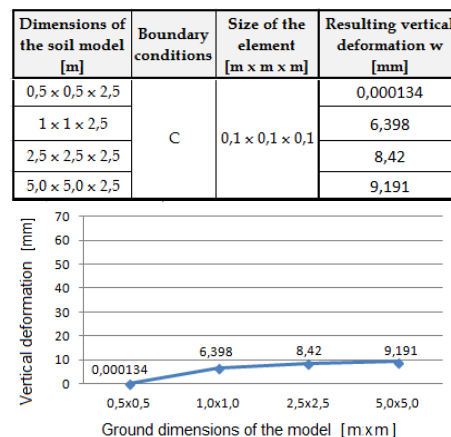


Fig. 16 Variant C – the resulting vertical deformation and vertical deformation vs. ground plan of the model

When the depth is 2.5 m and boundary conditions are D:

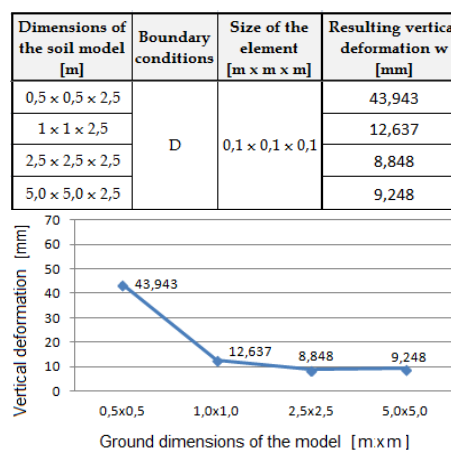


Fig. 17 Variant D – the resulting vertical deformation and vertical deformation vs. ground plan of the model

*D. Deformation vs. size of the 3D subsoil model*

The size of the model area was increased in the x, y, and z axes with same increments. In order to observe easily impacts of the increasing subsoil model, the ratios between the subsoil sizes was kept. The tables and charts below show the influence of the both ground plan dimensions and subsoil depths.

In case of A, deformation tended to increase with the increasing depth, while it decreased with the increasing ground plan size of the subsoil. But it is the depth which plays the key role for this variant.

Dimensions of the soil model [m]	Boundary conditions	Size of the element [m x m x m]	Resulting vertical deformation w [mm]
2,50 x 2,50 x 2,50	A	0,1 x 0,1 x 0,1	9,984
3,75 x 3,75 x 3,75			10,19
5,00 x 5,00 x 5,00			10,239

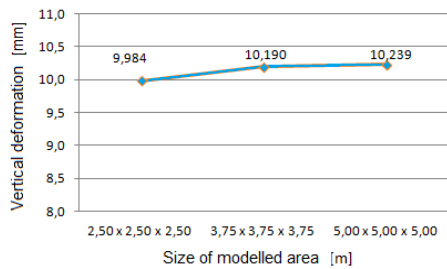


Fig. 18 Variant A - Vertical deformations vs. size of modelled area

For B, the depth is also more important than the ground plan size in terms of its influence on vertical deformation.

Dimensions of the soil model [m]	Boundary conditions	Size of the element [m x m x m]	Resulting vertical deformation w [mm]
2,50 x 2,50 x 2,50	B	0,1 x 0,1 x 0,1	8,848
3,75 x 3,75 x 3,75			9,430
5,00 x 5,00 x 5,00			9,669

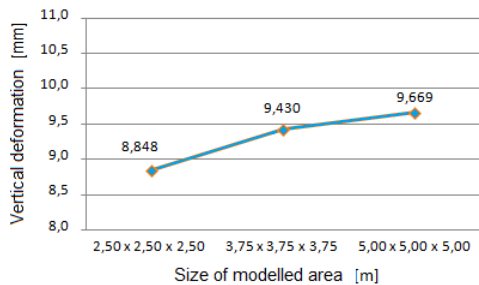


Fig. 19 Variant B - Vertical deformations vs. size of modelled area

In case of C, the depth almost did not influence the deformation.

With this variant, the key role is played by the grand plan – this means, by the boundary conditions which are defined on peripheral walls of the area.

Dimensions of the soil model [m]	Boundary conditions	Size of the element [m x m x m]	Resulting vertical deformation w [mm]
2,50 x 2,50 x 2,50	C	0,1 x 0,1 x 0,1	8,420
3,75 x 3,75 x 3,75			9,157
5,00 x 5,00 x 5,00			9,466

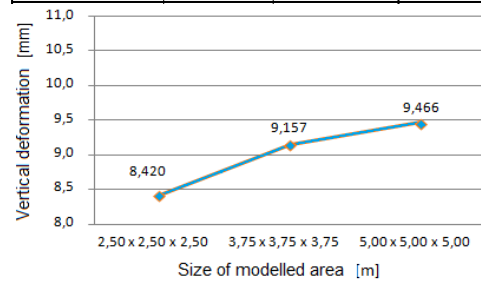


Fig. 20 Variant C - Vertical deformations vs. size of modelled area

For D - similarly as with A and B, it is rather the depth than the ground plan which influence more the vertical deformation.

Dimensions of the soil model [m]	Boundary conditions	Size of the element [m x m x m]	Resulting vertical deformation w [mm]
2,50 x 2,50 x 2,50	D	0,1 x 0,1 x 0,1	8,848
3,75 x 3,75 x 3,75			9,430
5,00 x 5,00 x 5,00			9,669

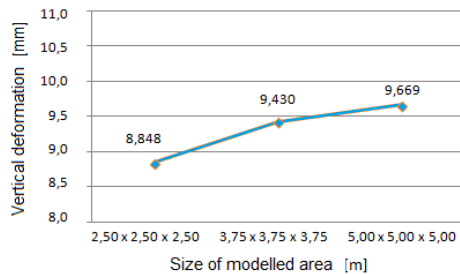


Fig. 21 Variant D - Vertical deformations vs. size of modelled area

*E. Final deformation of the plate*

Fig. 22 shows the final deformation of one of the model. The size of the subsoil and network were 2.5 x 2.5 x 2.5 m and 0.05 x 0.05 x 0.05 m, respectively. The boundary conditions were the D variant. The figure shows evident impacts of the boundary conditions which prevent external walls of the model to shift in horizontal directions and the base to shift vertically.

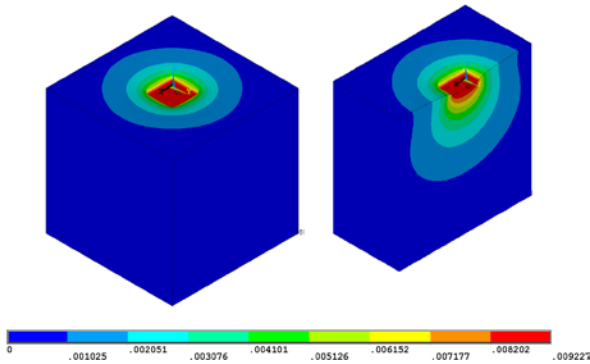


Fig. 22 Total deformation – a vertical section through subsoil (m)

Fig. 23 shows total deformation in a horizontal cross-section through the plate and subsoil. It is clear that the plate deformation above the subsoil is same as under the subsoil. In both cases, the maximum vertical deformation is 9.227 mm. The formation in a cross section is magnified so that the shape of the deformed concrete plate could be visible.

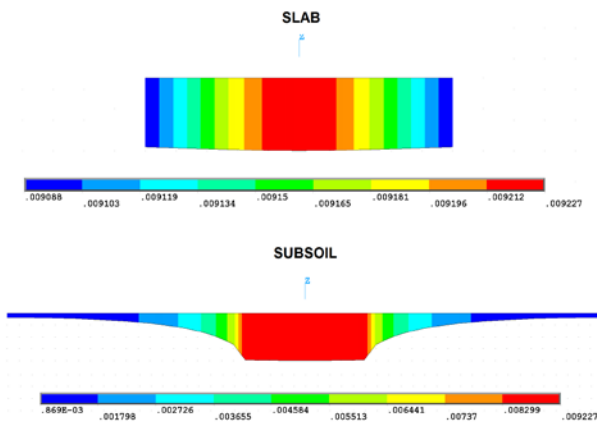


Fig. 23 Total deformation in a horizontal cross-section of the slab and subsoil (m)

Fig. 24 shows the total deformation in a vertical cross-section of the subsoil.

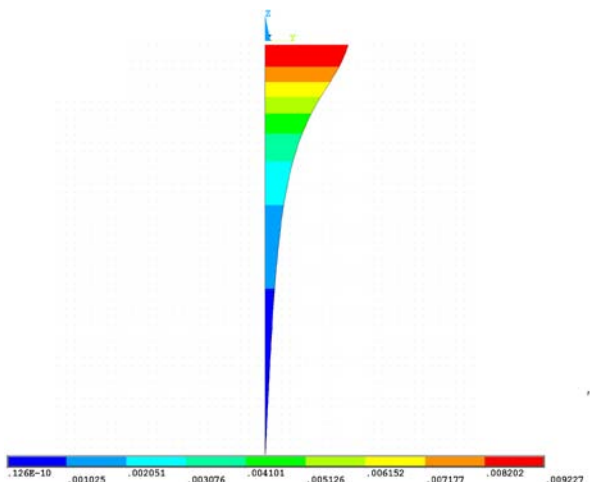


Fig. 24 Deformation along the subsoil depth - a vertical cross-section through the centre of the subsoil (m)

V. OTHER METHODS USED FOR CALCULATION OF THE RESULTING VERTICAL DEFORMATION

The task was also modelled in Scia Engineer 2009.0 using the 3D Soilin support. The Soilin module was used to calculate some parameters of the subsoil C. The module is based on the theory of an elastic semi-space defined by means of structural strength of soil. Gradually, subsidence incl. alternative rigidity of the soil C is calculated under the slab. Because the C parameters calculated in this way influence the contact stress which, in turn, influences subsidence of subsoil, an iterative calculation is used. In Scia Engineer the vertical deformation in the middle of the slab was  $w = 4.308$  mm.

The method required pursuant to the Czech standard ČSN 73 1001 is based on a modified elastic semi-space. Interaction with foundation is not considered. Using that method, the subsidence of subsoil under the centre of the slab was 7.086 mm.

The deformation in the middle of the slab measured during the experiment was ca. 3.7 mm.

VI. CONCLUSION

Fig. 25 shows impacts and relevance of the boundary conditions for the vertical deformation. The biggest difference in the vertical deformation for the increasing depths has been reached for A. In case of B and D, the horizontal deformation of subsoil’s external walls are prevented. This also influences the vertical deformation which is not as high as in A. In case of C, the boundary conditions of subsoil’s external walls play such a key role that the deformation almost does not depend on the depth.

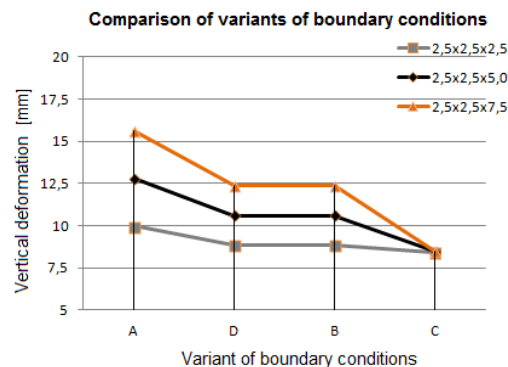


Fig. 25 Vertical deformation vs. boundary conditions

It follows from the characteristics deformation vs. variable depth of the subsoil model that the increasing depth results in linear increases in the vertical deformation. Considering different variants of the boundary conditions, one can compare the growth of vertical deformation once the depth becomes higher (Fig. 26).

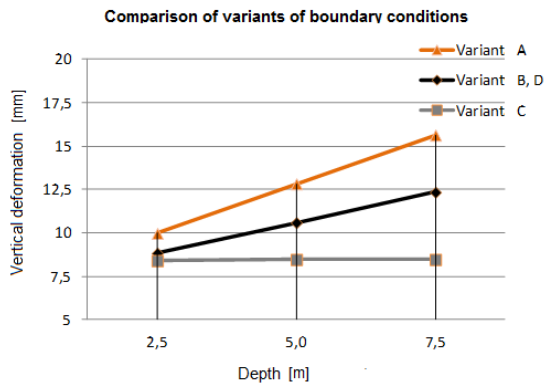


Fig. 26 Comparing the variants of boundary conditions – the resulting vertical deformation and the vertical deformation vs. depth

In case of the variant C when all walls except for the upper surface are fixed, the boundary conditions play such an important role that even the increasing depth does not increase the vertical deformation. On the other hand, the least influence of boundary condition has been witnessed for the variant A when deformation is possible for each wall of the subsoil model in each direction except for the lower base which is fixed. Fig. 26 shows that the higher the depth of the subsoil model is, the bigger the difference is between deformations calculated for the variants of boundary conditions. With the increasing depth of the subsoil model, the selection of boundary conditions is becoming a more important criterion which influences the final vertical deformation.

An important lesson learnt from characteristics describing the deformation versus variable size of subsoil ground plan is that the influence of any boundary condition is becoming weaker with the increasing ground plan of the subsoil. Using the chart in Fig. 27 it can be concluded that the boundary conditions play no role at all, if the ground plan of the subsoil model is big enough. Even in that case the boundary conditions influence the characteristics of the deformation versus the increasing depth of the subsoil which has been proved by the chart in Fig. 26.

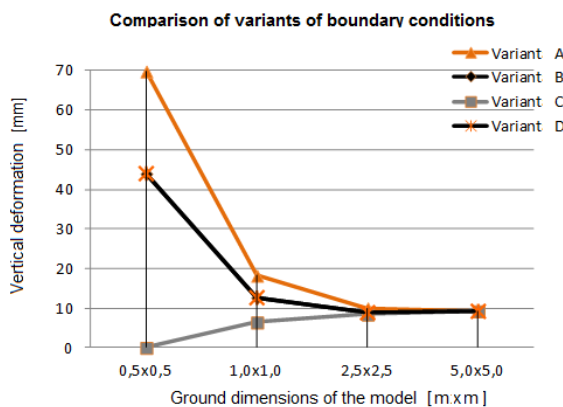


Fig. 27 Comparing the variants of boundary conditions – the resulting vertical deformation and the vertical deformation vs. ground plan of the model

It follows from Fig. 28 which shows the deformation vs. the

modelled area that the bigger is the area, the higher is the deformation. This is valid irrespective of the fact whether the primary reason for deformation is the depth of ground dimensions.

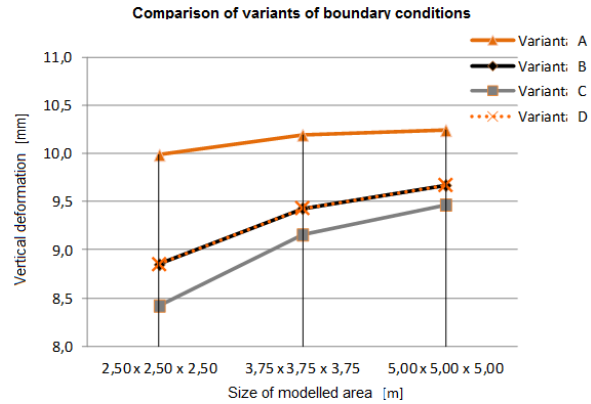


Fig. 28 Vertical deformation vs. the area size

The charts prove the major role played by the size of the model area and by the boundary condition itself. Results were quite scattered for the variants. Charts in Fig. 25, Fig. 26, Fig. 27, Fig. 28 indicate how the parameters of the area influence considerably the resulting vertical deformation.

Another important parameter which influences the final deformation is the degree of discretising. Division of the model into finite elements influences both the results and the number of degrees of freedoms, being thus important for the calculation time and quantity of processed data.

168 different models were create din ANSYS for interaction between subsoil and plain concrete slab. The models used different boundary conditions, size of the modelled area and size of the finite element network. Some models were linear, while the others non-linear.

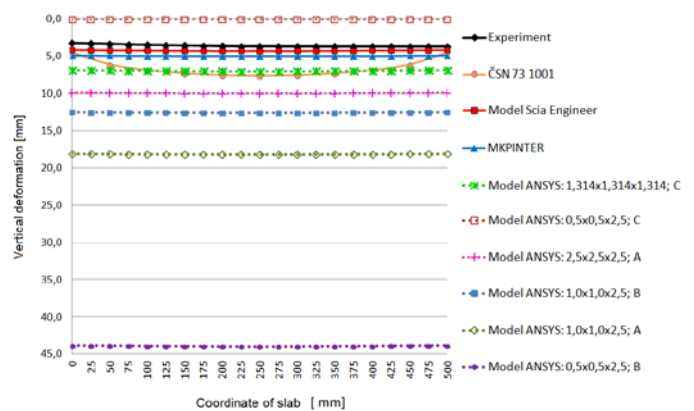


Fig. 29 Comparing the variants of boundary conditions – the resulting vertical deformation and the vertical deformation vs. ground plan of the model

When comparing these values with the similar values of deformation obtained by other methods, the conclusion can be drawn that the values of deformation resulting from the 3D model are too scattered. In this set of results, the vertical deformation is  $w = 6.398$  mm which approaches most the final

deformation measured during the experiment (cca 3.70 mm). Fig. 29 shows the values obtained in the model in Scia Engineer where the vertical deformation in the middle of the slab was  $w = 4.308$  mm. The chart in Fig. 29 also shows the vertical deformation calculated in the method required by ČSN 73 1001 – in that case the deformation is 7.086 mm under the centre of the slab.

There can be many different reasons for deviations between the calculated and measured quantities, for instance, uncertainties resulting from determination of geomechanic properties of subsoil or climatic influences.

#### ACKNOWLEDGMENT

This outcome has been achieved with the financial support by the project “Conceptual development of science and research activities 2014” on the Faculty of Civil Engineering, VSB-TU Ostrava.

#### REFERENCES

- [1] R. Cajka, P. Manasek, , Building Structures in Danger of Flooding. *IABSE Conference New Delhi, India 2005: Role of Structural Engineers towards Reduction of Poverty*. New Delhi, India, pp. 551-558 ISBN 978-3-85748-111-6, WOS: 000245746100072, (2005).
- [2] R. Cajka, Determination of Friction Parameters for Soil – Structure Interaction Tasks. *Recent Researches in Environmental & Geological Sciences. Energy, Environmental and Structural Engineering Series No. 4*, pp. 435-440. *Proceedings of the 7th WSEAS International Conference on Continuum Mechanics (CM '12)*. Kos Island, Greece, July 14-17, 2012, pp. 435-440, ISSN 2227-4359, ISBN 978-1-61804-110-4
- [3] R. Cajka, General Contact Element using Jacobian of Transformation and Gauss Numerical Integration of Half-space. *In Proceedings of the 3rd International Conference on Mathematical Models for Engineering Science (MMES'12)*, WSEAS Press, Paris, France, December 2-4, 2012, pp. 23-28, ISBN 978-1-61804-141-8
- [4] R. Cajka, J. Labudkova, Influence of parameters of a 3D numerical model on deformation arising in interaction of a foundation structure and subsoil. *1st International Conference on High-Performance Concrete Structures and Materials (COSTMA '13)*. Budapest, Hungary, December 10-12, 2013, ISSN 2227-4359, ISBN 978-960-474-352-0
- [5] R. Cajka., P. Mateckova, Temperature Distribution of Slide Joint in Reinforced Concrete Foundation Structures. *17th International Conference on Engineering Mechanics 2011*, Svratka, May 09-12, 2011. *Engineering Mechanics 2011*, pp. 95-98, ISBN 978-80-87012-33-8, WOS: 000313492700017
- [6] R. Cajka, P. Mateckova, M. Janulikova, Bitumen Sliding Joints for Friction Elimination in Footing Bottom. *Applied Mechanics and Materials*, Volume 188, (2012), pp. 247-252, ISSN: 1660-9336, ISBN: 978-303785452-5, DOI: 10.4028/www.scientific.net/AMM.188.247
- [7] R. Cajka., V. Krivy, D. Sekanina, Design and Development of a Testing Device for Experimental Measurements of Foundation Slabs on the Subsoil. *Transactions of the VSB - Technical University of Ostrava, Construction Series*, Volume XI, Number 1/2011, VSB - TU Ostrava, Pages 1–5, ISSN (Online) 1804-4824, ISSN (Print) 1213-1962. DOI: 10.2478/v10160-011-0002-2, 2011.
- [8] R. Cajka, Accuracy of Stress Analysis Using Numerical Integration of Elastic Half-Space (2013). *Applied Mechanics and Materials*, 300-301, pp. 1127-1135. ISSN: 16609336, ISBN: 978-303785651-2, DOI: 10.4028/www.scientific.net/AMM.300-301.1127
- [9] R. Cajka, K. Burkovic, R. Fojtik, Experimental Soil – Concrete Plate Interaction Test and Numerical Models. *Key Engineering Materials*, Vols. 577-578, (2014), pp 33-36, doi:10.4028/www.scientific.net/KEM.577-578.33
- [10] R. Cajka, R. Fojtik, Development of Temperature and Stress during Foundation Slab Concreting of National Supercomputer Centre IT4, *Procedia Engineering*, Volume 65, 2013, Pages 230-235, ISSN 1877-7058, doi: 10.1016/j.proeng.2013.09.035
- [11] R. Cajka, Horizontal Friction Parameters in Soil – Structure Interaction Tasks. *Advanced Materials Research*, Vol. 818 (2013), pp 197-205, Trans Tech Publications, Switzerland, doi:10.4028/www.scientific.net/AMR.818.197
- [12] R. Cajka, Analysis of Stress in Half-space using Jacobian of Transformation and Gauss Numerical Integration. *Advanced Materials Research*, Vol. 818 (2013), pp 178-186, Trans Tech Publications, Switzerland, doi:10.4028/www.scientific.net/AMR.818.178
- [13] R. Cajka, P. Labudek, K. Burkovic, M. Cajka, Golf Club Structure and Foundation with Slide Joint on the Undermined Territory. *6th WSEAS International Conference on Engineering Mechanics, Structures, Engineering Geology (EMESEG '13)*, WSEAS / NAUN International Conferences, Cambridge, UK, February 20-22, 2013, ISSN 2227-4588, ISBN 978-1-61804-165-4
- [14] J. Halvonik, L. Fillo, The Maximum Punching Shear Resistance of Flat Slabs, *Procedia Engineering*, Volume 65, 2013, Pages 376-381, ISSN 1877-7058, doi: 10.1016/j.proeng.2013.09.058.
- [15] T. Janda, M. Sejnoha, J. Sejnoha, Modeling of soil structure interaction during tunnel excavation: An engineering approach. *Advances in Engineering Software*, 62-63, pp. 51-60., doi: 10.1016/j.advengsoft.2013.04.011
- [16] M. Janulikova, M. Stara, Reducing the Shear Stress in the Footing Bottom of Concrete and Masonry Structures, *Procedia Engineering*, Volume 65, 2013, Pages 284-289, ISSN 1877-7058, doi: 10.1016/j.proeng.2013.09.044.
- [17] J. Kralik, Optimal design of NPP containment protection against fuel container drop. *Advanced Materials Research*, Vol. 688, 2013, pp. 213-221, Trans Tech Publications, Switzerland, DOI: 10.4028/www.scientific.net/AMR.688.213
- [18] J. Labudkova, Comparison of soil - foundation interaction models with measured values, *MSc. Thesis*, Vol. 163, VSB – TUO, Ostrava, 2013.
- [19] P. Mynarcik, Technology and Trends of Concrete Industrial Floors, *Procedia Engineering*, Volume 65, 2013, Pages 107-112, ISSN 1877-7058, doi: 10.1016/j.proeng.2013.09.019.
- [20] M. Stara, M. Janulikova, Laboratory Measurements and Numerical Modeling of Pre-stressed Masonry, *Procedia Engineering*, Volume 65, 2013, Pages 411-416, ISSN 1877-7058, doi: 10.1016/j.proeng.2013.09.064.
- [21] K. Frydrysek, R. Janco, H. Gondek, Solutions of Beams, Frames and 3D Structures on Elastic Foundation Using FEM. *International Journal of Mechanics*, Issue 4, Volume 7, 2013, pp. 362-369
- [22] O. Sucharda, J. Brozovsky, Bearing Capacity Analysis of Reinforced Concrete Beams. *International Journal of Mechanics*, Issue 3, Volume 7, 2013, pp. 192-200
- [23] I. Racanel, Design of Bridge Shallow Foundations Using Finite Element Method (2013). *Recent Advances in Civil and Mining Engineering*, pp. 23 – 29. *Proceedings of the 4th European Conference of Civil Engineering (ECCIE '13). Proceedings of the 1st European Conference of Mining Engineering (MINENG '13)*. Antalya, Turkey, October 8-10, 2013, ISSN: 2227-4588, ISBN: 978-960-474-337-7.
- [24] R. Cajka, K. Burkovic, V. Buchta, Foundation slab in interaction with subsoil. *Advanced Materials Research. Volume 838-841*, 2014, Pages 375-380, ISSN: 10226680 ISBN: 978-303785926-1, DOI: 10.4028/www.scientific.net/AMR.838-841.375.
- [25] V. Buchta, P. Mynarcik, Experimental testing of fiberconcrete foundation slab model, *Applied Mechanics and Materials*, Volume 501 – 504 (2014), Pages 291-294, Trans Tech Publications, Switzerland, doi:10.4028/www.scientific.net/AMM.501-504.945.
- [26] J. Krizek, Soil-structure interaction of integral bridges (2011), *Journal of the International Association for Bridge and Structural Engineering (IABSE)*, 21 (2), pp. 169-174, ISSN: 10168664, DOI: 10.2749/101686611X12994961034372
- [27] A.V. da Fonseca, Load tests on residual soil and settlement prediction on shallow foundation (2001), *Journal of Geotechnical and Geoenvironmental Engineering*, 127 (10), pp. 869-884, doi: 10.1061/(ASCE)1090-0241(2001)127:10(869)
- [28] K.C. Foye, P. Basu, M. Prezzi, Immediate settlement of shallow foundations bearing on clay (2008), *International Journal of Geomechanics*, 8 (5), pp. 300-310, doi: 10.1061/(ASCE)1532-3641(2008)8:5(300)